Plasmonic Coupling and Long-Range Transfer of an Excitation along a DNA Nanowire

J. Jussi Toppari,[†,‡] Janina Wirth,[‡] Frank Garwe,[‡] Ondrej Stranik, Andrea Csaki, Joachim Bergmann, Wolfgang Paa, and Wolfgang Fritzsche[*]

Institute of Photonic Technology, Albert-Einstein-Strasse 9, Jena 07745, Germany. [‡]These authors contributed equally. [†]Present address: Nanoscience Center, Department of Physics, P.O. Box 35, 40014, University of Jyväskylä, Finland.

ABSTRACT We demonstrate an excitation transfer along a fluorescently labeled dsDNA nanowire over a length of several micrometers. Launching of the excitation is done by exciting a localized surface plasmon mode of a 40 nm silver nanoparticle by 800 nm femtosecond laser pulses *via* two-photon absorption. The plasmonic mode is subsequently coupled or transformed to excitation in the nanowire in contact with the particle and propagated along it, inducing bleaching of the dyes on its way. *In situ* as well as *ex situ* fluorescence microscopy is utilized to observe the phenomenon. In addition, transfer of the excitation along the nanowire to another nanoparticle over a separation of 5.7 μm was clearly observed. The nature of the excitation coupling and transfer could not be fully resolved here, but injection of an electron into the DNA from the excited nanoparticle and subsequent coupled transfer of charge (Dexter) and delocalized exciton (Frenkel) is the most probable mechanism. However, a direct plasmonic or optical coupling and energy transfer along the nanowire cannot be totally ruled out either. By further studies the observed phenomenon could be utilized in novel molecular systems, providing a long-needed communication method between molecular devices.

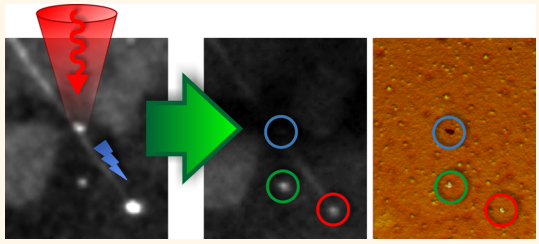

KEYWORDS: DNA · nanoparticle · surface plasmon · energy transfer · femtosecond laser pulse

The ever-growing progress of micro- and nanotechnology, which has influenced vast aspects of our lives and cultures (information and communication technology, entertainment, *etc.*) during the last decades, is crucially related to the increasing miniaturization of electronic devices. However, the development of the established *top-down* fabrication technologies is already slowing down, and substantial barriers to further progress are encountered both in the operation of devices and even more in a cost-efficiency of the fabrication. Thus, in order to ensure the continuation of Moore's law and especially to discover novel new fabrication methods for realization of the inexpensive mass production in nanoscale, many *bottom-up* technologies have been developed during the past decade. These methods are relying on totally opposite processes, such as chemical synthesis and in particularly self-assembly, for which one of the most studied and promising molecules is DNA. Its superior self-assembly properties have been proven by many different constructions, such as tile-based arrays,[1] origami structures,[2,3] and recently even 3D-origami.[4] In addition, DNA has been predicted to serve as a good conductor,[5−8] but so far the experimental results have been highly controversial and diverging.[9,10] This has been assigned mainly to the fragility of the double-stranded DNA (dsDNA) against the environment,[11−16] especially in light of recent results showing that within a well-controlled environment a real charge transfer (CT) exists in the double helix.[16,17] Due to this, a number of supposedly better DNA-based conductors have been developed, *e.g.*, M-DNA[18,19] and G4-wires,[20,21] which are also more robust. However, the long-range conductivity is still an open question.

Although an impressive variety of molecular assemblies, DNA based as well as others, is accessible already, there still exists a major obstacle: The difficulty of integration of such devices into the present technological environments. Especially, realization of a proper electrical connection to a molecule is challenging. For that, chemical affinity- and electric field-based linking, for example, have been suggested, but so far they have not proven their full potential, mostly due to the high contact resistances induced by

* Address correspondence to wolfgang.fritzsche@ipht-jena.de.

Received for review October 16, 2012 and accepted January 10, 2013.

Published online January 10, 2013
10.1021/nn304789w

mismatches between the molecular levels and the Fermi level of the metal or the band structure of a semiconductor, which are difficult to control.[22] Another widely suggested interconnection technology is based on optical coupling, *i.e.*, using light irradiation to switch the state (electrical or conformational) of an absorbing structure.[23,24] Yet, the immediate disadvantage of this approach would be the restriction of the miniaturization to the diffraction limit defined by wavelength.

However, plasmonics, based on propagating or localized surface plasmon polaritons (SPP), *i.e.*, the strongly coupled excitations of electromagnetic field and oscillation of free electrons on metal, could provide a robust optical-like connection while overcoming the diffraction limit.[25,26] By the localized SPP resonance (LSPR) appearing on metallic nanoparticles (NPs),[27,28] optical energy can be directed even down to subwavelength volumes, as demonstrated by using the high electric field of LSPR to destroy the nearest surroundings of NPs within biological systems, such as cells,[29,30] metaphase chromosomes,[31] and protein aggregates[32] or in technical materials such as PMMA.[33] These effects are mostly based on a local heating[29−32] or emission of electrons overcoming the work function of the metal *via* multiphoton absorption.[33−36] However, by combining LSPR with a nanoantenna effect[37,38] or utilizing optically active molecules[39] even a real optical access to subwavelength structures can be realized. Although this has been already demonstrated for some discrete systems, interconnections between several functional units on the surface must still be realized. So far, these interconnections have been demonstrated only by metallic strips, not providing parallel fabrication and again limited by top-down miniaturization problems as discussed before.[39−41]

More interestingly, an excited LSPR can also couple the excitation energy directly to a molecular wire, where it propagates further, as was demonstrated for the first time in our previous study of a nanometer-wide destruction of a PMMA film along a dsDNA excited *via* NPs.[42] If this effect could be thoroughly understood and utilized, a new world of optoelectronic circuitry would be accessible with the potential to address the needs of future development. In this article we use fluorescence as a more precise local tool to study this phenomenon and the nature of the propagating excitation: electrical (CT) or plasmonic/optical. We demonstrate the excitation transfer over several micrometers along a fluorescently labeled dsDNA-based molecular wire upon plasmonic excitation of a silver nanoparticle (AgNP) in contact with it. Furthermore, we demonstrate a transport of the excitation along the wire to another nanoparticle several micrometers away, thus establishing a link between the nanoparticles by combining the advantages of both the molecular assemblies and plasmonics. By utilizing this phenomenon on communication between novel molecular devices, real nanoscale integration with bottom-up fabrication capabilities could be realized. However, further studies are still needed to reveal the fundamental nature of the propagating excitation and, for example, to prevent the destruction of the AgNPs used for excitation.

RESULTS AND DISCUSSION

Molecular wires used in the experiments consisted of genomic bacteriophage λ-DNA molecules fluorescently stained with an intercalating dsDNA-specific SYBR green II dye, bundled together and elongated on a glass substrate covered with PMMA, by the receding meniscus of a drying droplet.[43−45] The number of dsDNA molecules per bundle varied from two to around 10. Plasmonic coupling was realized *via* chemically synthesized AgNPs with a diameter of ~40 nm and the resulting LSPR band around 417 nm.[46] The SYBR green II dye was chosen due to its distinct absorption and excitation maxima at 488 nm and at 266 nm, which is the third harmonic of the utilized 800 nm laser. The observed contrast in the fluorescence between the presence and the absence of dsDNA was more than a factor of 100, which is important for a reduction of the background. The fluorescent and absorption properties of the nanoparticles and the dye are presented in more detail in the Supporting Information.

The excitation transfer was initiated by illuminating the AgNP attached to a DNA wire, by 100 fs long laser pulses at a wavelength of 800 nm. Although neither the DNA, the dye, nor the AgNPs are active at this wavelength, the high electric fields of the femtosecond laser can excite plasmonic modes in the AgNPs *via* multiphoton absorption enabled by the plasmonic field enhancement.[47] Thus, this provides a real nanoscale spatial confinement for the initiation, as all the excitations of the DNA or the dye must happen *via* the localized LSPR modes of the AgNP excited by second (400 nm), third (266 nm), or higher order processes of the illumination wavelength. It should be stressed that the absorption and thus the excitation strength of the dye is very low at 400 nm but high at 266 nm (see the Supporting Information). Figure 1 represents schematics of the utilized setup. More details can be found in the Methods section.

After fabrication, the sample was characterized by atomic force microscopy (AFM) to find suitable isolated molecular wires connected with AgNPs. (Typical AFM images are presented in Figures 2 and 3.) In addition, before and after the laser excitation a fluorescence image was taken of the studied sample by illuminating it with 470 nm light and recording the fluorescence at 550 nm by a CCD camera, as shown in Figure 1. A fluorescence image of a single molecular wire with a small aggregate of nanoparticles attached in the middle is presented in Figure 2A. As seen from the image, AgNPs are highly fluorescent, which implies that

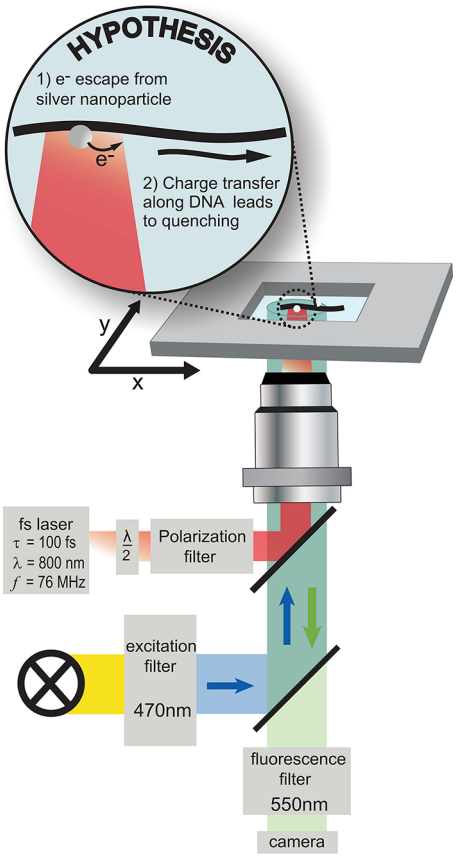

Figure 1. Schematics of the measurement setup and the observed phenomenon. The excitation of the silver nanoparticle was done by the fs laser while simultaneously imaging the fluorescence with the CCD camera. For pure fluorescence imaging, white light through the excitation filter was used for illumination. It should be noted that the laser and the white light excitation were never used simultaneously.

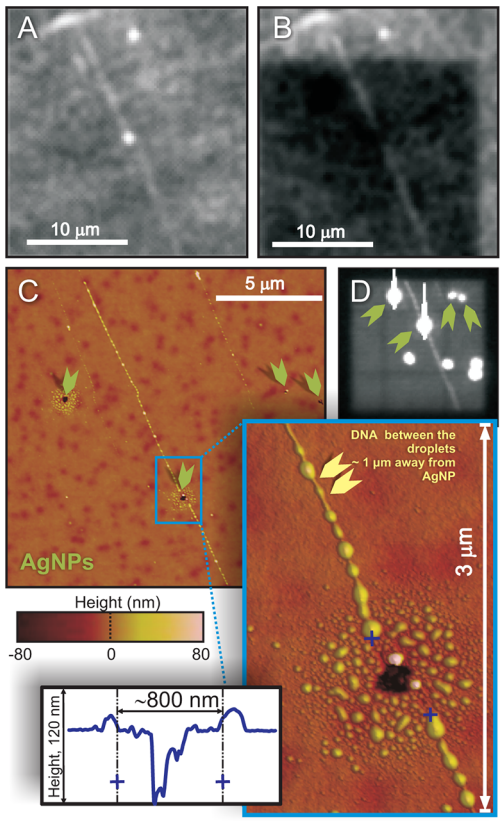

Figure 2. Experiment on a DNA nanowire with an attached AgNP. (A) Fluorescence image of a sample before the laser illumination showing a DNA nanowire with a bright AgNP in the middle. (B) Fluorescence image of the same sample after the scanning fs-laser illumination. The illuminated area is clearly visible as a darker region. The fluorescence of the excited nanoparticle has disappeared, and the dye on the DNA wire has been bleached around it. (C) AFM height image showing the DNA nanowire and the AgNP after the laser illumination. The height color scale is shown below, and the green arrows point to holes left by the destroyed nanoparticles. The zoomed area (blue rectangle) shows an enhanced view of the excited AgNP, revealing destruction of the particle and the DNA close to it, as well as the PMMA below them (visible as dark ~80 nm deep holes/wells[42]), over a 800 nm range, as shown by the cross-section taken *via* the blue crosses. However, the DNA looks intact further away. This destruction cannot be due to a simple thermal effect as explained in the text. The droplets along the DNA are probably moisture gathered from air or left from the buffer while drying. (D) Overlaid fluorescent images taken during the fs-laser illumination. The excited AgNPs are visible as bright spots. AgNPs pointed out by the green arrows were destroyed during the laser illumination, visible in the AFM image (C) as ~80 nm deep holes in the PMMA. Other particles are out of the AFM image range.

the SYBR green II attaches to them also. The reason for the observed increased fluorescence even when the dyes attached to AgNPs are not intercalated can be due to a very efficient and dense attachment or plasmonic enhancement of the dye excitation. Also some background is visible despite the high contrast of the intercalated dye compared to free dye.

After fluorescent imaging the nanoparticles were excited by scanning the femtosecond laser with a focus width of 2 μm, a pulse fluence of ~3 mJ/cm^2, and a repetition rate of 76 MHz, over the sample in 1 μm steps. The scanning was done by the sample stage within a 20 μm × 20 μm area containing the nanoparticle of interest, thus ensuring excitation at least on one of the illumination points. The laser illumination was continued for one second per position, and during the stage movements the beam was shut by an electronic shutter. On each illumination position, the whole sample was also simultaneously imaged by the CCD camera through the same 550 nm fluorescent filter, to observe the fs-laser-induced fluorescence. To ensure detection of the possible very weak signals, the camera was operated in electron multiplication mode, allowing even single photon detection. Figure 2D presents the images recorded during the laser scanning, overlaid over the whole scanned area of the same sample as in Figure 2A. Faint background visible everywhere indicates very weak direct excitation of the dye by the 800 nm laser pulses or a third-harmonic generation (THG) somewhere inside the sample. The DNA wire is clearly visible mostly due to the much higher fluorescence of the intercalated dye compared to the free dye

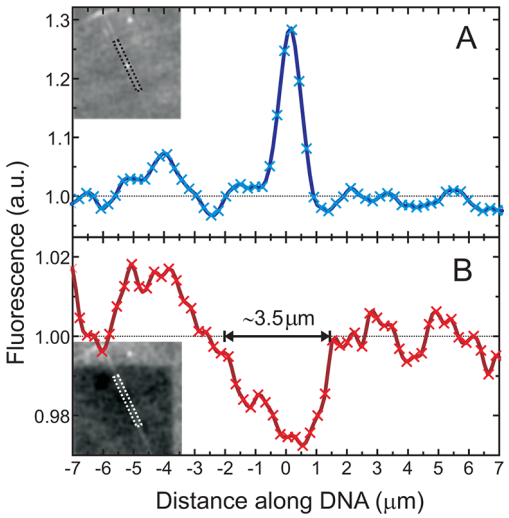

Figure 3. Bleaching along the DNA nanowire induced by the excited AgNP. Cross-section of the fluorescence profile before (A) and after (B) the laser illumination. The cross-sections have been taken along the area shown in the insets (same fluorescence images as in Figure 2A and B) by averaging the width of the area at each distance along the DNA. AgNP is situated on the origin of the graphs.

(see Supporting Information), but the excitation of the dye on the dsDNA could also be selectively enhanced by THG.[48−51]

All AgNPs within the scanned area show up as extremely bright spots, even saturating the CCD when hit by the laser pulses, as illustrated by arrows in Figure 2D. This clearly shows that the dyes attached to the AgNPs are efficiently excited *via* three-photon excitation enabled by the plasmonic modes of the particle. However, none of the individual images showed any fluorescence along the DNA nanowire during the fs-laser illumination of the AgNP, as would have been expected if the excitation travels as light or plasmonic exciton with energy similar to 266 nm light. The reason could be too weak fluorescence masked by the bright fluorescence of the AgNP or the absence of fluorescence at all.

After the fs-laser illumination, a new fluorescence image was taken as shown in Figure 2B for the same sample. The laser-illuminated area is clearly visible as a darker region due to bleaching of the dye. From the image one can see that the dye on the nanoparticle has been totally bleached, as well as the dye intercalated on the DNA wire around it. However, everywhere else the DNA wire looks intact. An AFM height image from the same sample after the laser illumination is shown in Figure 2C with the AgNP of interest zoomed on the blow-up. Due to the high excitation by the fs-laser pulses, all the laser-illuminated AgNPs (shown by green arrows) have been destroyed as well as the PMMA under them, leaving ~80 nm deep holes on the PMMA layer, as seen from the image.[42,47] Like in the previous observations, the DNA attached to the AgNP, and also the PMMA below it, was destroyed within a length of ~400 nm away from the particle.[42] This can be verified from the blow-up AFM image of Figure 2C and the attached cross-section taken from it. The observed "bumps" along the DNA are probably moisture droplets gathered from air or left from the drying of the buffer.

Further, by taking cross-sections of the fluorescence images (Figure 2A and B) along the DNA nanowire, as shown in Figure 3, one can see that the bleaching of the fluorescence has taken place over a far longer range than the destruction of the DNA, *i.e.*, at least over the range of ~1.5 μm away from the particle. This indicates the propagation of the excitation along the DNA much farther than would be expected by the destruction. To ensure that the bleaching of the dye is really attributed to the coupling of the excitation into the DNA *via* LSPR of the AgNP, the same experiment was repeated with a similar DNA nanowire, but now with a nanoparticle located 780 nm away from it. Similar high fluorescence of the nanoparticle during the laser illumination was observed, as well as destruction of it on the AFM image afterward. However, the fluorescence of the DNA was not affected, since the distance to the particle was so long that its plasmonic field on the wire is negligible. Results are shown in the Supporting Information.

This proves that the close proximity or even a direct contact between the DNA wire and AgNP is needed for the coupling, which further implies the effect being launched by the plasmonic excitation in AgNP. However, this does not yet fully rule out the simple possibility that the bleaching of the dye along the DNA would be due to a local heating of the particle during the illumination. Nevertheless, our earlier studies have shown that illumination by femtosecond pulses with similar fluencies to those here induces a maximal temperature increase of only 10 K (10 nm below the particle) and an accumulated temperature rise of about three degrees within a few nanometers from the particle,[33] which is not enough to cause the bleaching of the dye along the DNA. Also, the sinking of a nanoparticle into PMMA, as we observe in our experiments, requires nanoparticle temperatures higher than 400 °C and a large force on them over a few nanoseconds.[52] Thus, the observed phenomenon cannot be just due to a simple thermal effect.

As the simple thermal effect is ruled out, there are still a few possibilities for the nature of the excitation. The propagating excitation could be optical, assuming the DNA bundles behave as subwavelength optical fibers (fibers smaller than 50 nm have been demonstrated[53]) to where the light from the SPP modes of the nanoparticle could scatter. Also a plasmonic nature is conceivable, in which case the excitation would propagate through the DNA as quasi-particles, called excitons.[54,55] However, since the initial excitation happens *via* three-photon absorption enabled by the

LSPR of the AgNP, both of these methods should involve an optical excitation with 266 nm wavelength and thus fluorescence of the dye along the propagation, which was not observed. Anyway, we cannot totally rule out these choices, as the fluorescence could have been too weak or masked by the bright luminescence of the AgNp, as discussed before.

Most probably the observed bleaching of the dye along the DNA nanowire is due to a coupled transfer of charge (Dexter) and faster delocalized exciton (Frenkel) along the DNA.[55] Sole charge transfer has been proven for short dsDNAs, and the coupled Dexter and Frenkel transfer is feasible for a longer range within DNA bundles or similar constructions.[13,16,56] As the femtosecond laser irradiation causes a very high plasmonic excitation on the AgNPs with highly enhanced electric fields, the excited electrons in the nanoparticles can overcome the work function by absorption of multiple photons,[34,35] which leads to Coulomb explosion.[36] These processes start at a laser fluence around 3 to 7 mJ/cm^2. The escaped electrons can subsequently be injected on empty electronic states or excite other electrons on DNA. This excess charge can further propagate along the DNA, leading to a bleaching or quenching of the intercalated dye without fluorescence.[57,58] The longer propagation of the coupled charge (short-range) and Frenkel excitons (long-range) along the DNA can be sustained by the initial kinetic energy of the escaped electron, which can be as high as 50 eV.[34] Or, it can be driven by the very high electric field of the fs-laser pulses, present several micrometers away from the AgNP, possibly leading to a directional net effect *via* second-order processes; even the kinetic effect of the fundamental alternating laser field averages to zero.[48−50]

To further prove the discussed excitation transfer, we utilized a sample with two separate small aggregates of dye-labeled AgNPs attached to the same dsDNA nanowire with intercalated dye. The separation of the AgNP aggregates was ~5.7 μm, as shown by the fluorescence image of the sample in Figure 4A. The image was taken similarly to the case of one AgNP above. The fs-laser illumination area was now chosen so that from the two AgNP aggregates on the same nanowire only the upper one (blue box in Figure 4) could be excited during the scanning process. The scanning was done exactly the same way as described above except the illumination time per pixel was 500 ms this time. The fluorescence image (Figure 4B) taken after the illumination shows again bleaching of the dye on the excited AgNPs, as well as of the intercalated dye along the DNA starting from the excited nanoparticle. Also other particles within the illumination area were bleached. In addition and more interestingly, the dye on the other AgNP aggregate attached to the end of the same DNA (red box in Figure 4) was also significantly bleached, although it was not excited by the fs laser at any time. This means

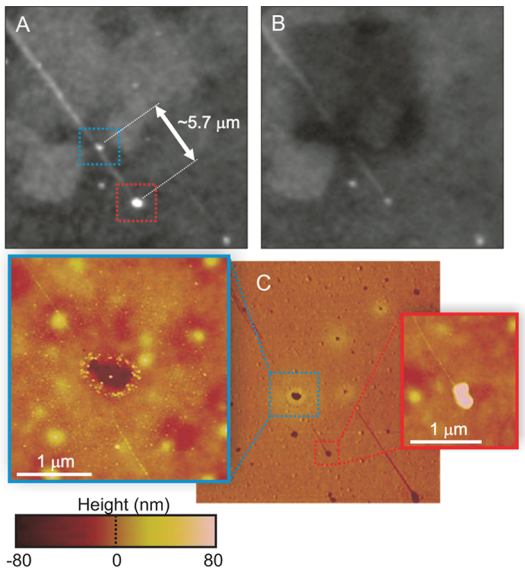

Figure 4. Experiment on a DNA nanowire with two attached AgNPs demonstrating the excitation transfer along the wire. Fluorescence images of the sample with two aggregates of nanoparticles, marked with blue (donor) and red (acceptor) boxes, before (A) and after (B) the point by point fs-laser illumination within an area including the donor but not the acceptor AgNP (visible as a darker rectangular on B). At the place of the donor only a dark region is visible in B, similarly to that for other illuminated AgNPs within the illumination area. Also the fluorescence of the acceptor outside the illumination area, is clearly bleached. Separation of the donor and acceptor particles is 5.7 μm. (C) AFM phase image of the nanoparticles and the connecting DNA wire after the fs-laser illumination. The blow-ups are zoomed height images of the donor and acceptor nanoparticles, with the height color scale shown below.

that the excitation (charge or energy on optical range) from the excited nanoparticle (donor) needed to be transferred along the DNA nanowire all the way to the other AgNP (acceptor) to induce bleaching.

From the AFM images taken after the laser illumination and shown in Figure 4C, one can see that again the excited donor nanoparticle (blue box) was destroyed by the laser illumination, as also the DNA in the vicinity of the particle and PMMA below them. Also, by comparing Figure 4B and 4C, one can see that all the AgNPs within the fs-laser illumination area have been destroyed. However, the not-excited but still bleached acceptor AgNP (red box) looks intact on the AFM image, further proving that the bleaching of the dye on it was not due to a direct plasmonic excitation by the laser focus wings.

A more quantitative analysis of this experiment is presented in Figure 5, where a fluorescence cross-section along the DNA nanowire covering both the donor (at position ~1.5 μm) and the acceptor (at position ~7.2 μm) AgNPs is plotted before (blue curve) and after (red curve) the laser illumination. The obtained result shows a clear bleaching of the dye on the excited donor AgNP, as well as of the intercalated dye along the DNA near it. However, even when the bleaching of the intercalated dye has stopped around three micrometers

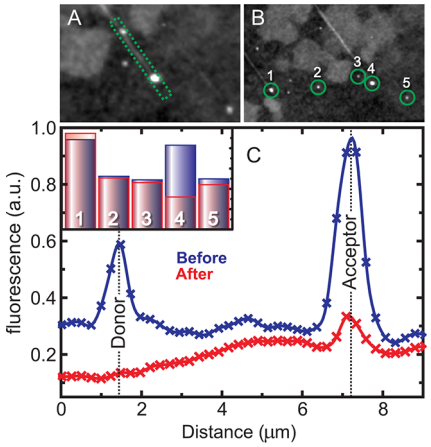

Figure 5. Measured fluorescence in the experiment on a DNA nanowire with two attached AgNPs. (C) Fluorescence along the DNA nanowire, *i.e.*, along the area shown as a green rectangle in (A) by averaging the width of the area at each point along the DNA. Both the donor and the acceptor AgNPs are clearly visible before the illumination (blue curve). After the illumination (red curve) the donor is totally bleached and the acceptor is clearly also. (C, inset) Fluorescence of the dye on several AgNPs, numbered 1−5 in (B), before (blue) and after (red) the fs-laser illumination. The fluorescence has been measured as an integral over the green circles in (B) including the particles (1−5). Particle 4 is the acceptor AgNP, and it shows a clear bleaching compared to other AgNPs. The fluorescence images (A) and (B) are the same as in Figure 4A, except showing a narrower and wider area, respectively.

from the donor particle, the dye on the acceptor still shows a significant bleaching. This proves that the charge or energy of the induced excitation has indeed traveled *via* the DNA nanowire from the donor AgNP to the acceptor 5.7 μm away and that the excitation transfer happens even further than shown by the bleaching of the intercalated dye.

In addition, to rule out possible effects by a general bleaching due to fluorescent imaging or small changes on the focus, the fluorescence of several isolated dye-labeled AgNPs (NPs 1−3 and 5 in Figure 5) as well as the acceptor AgNP at the end of the DNA wire (NP 4; red box) were compared before and after the laser illumination, as also shown in Figure 5. All the examined particles are located outside of the laser illumination area and thus were not excited by the fs laser. Their initial fluorescence varies due to different sizes and amounts of attached dye. Since the particles 1−3 and 5 are not connected to the donor by any nanowire, they act as controls. From the data (Figure 5) it is clear that dye on the acceptor AgNP (4) has been severely bleached compared to the control AgNPs. The observed bleaching is more than 10 times higher than any measurement uncertainties (see *e.g.* fluorescence of AgNPs 1 and 5) and thus clearly not due to a general bleaching induced by the imaging or differences in focusing or any other random differences during the imaging.

CONCLUSIONS

We have shown that excitation can be coupled from the LSPR modes of a silver nanoparticle excited *via* multiphoton absorption by a femtosecond laser pulse, to the attached DNA nanowire, and that the excitation can be transferred along the nanowire for distances of several micrometers. The transfer along the DNA wire was demonstrated nondestructively by bleaching of the SYBR green II dye intercalated into the DNA. Furthermore, we have demonstrated a transport of this excitation from a nanoparticle to another nanoparticle ~5.7 μm away along a DNA nanowire connecting them. The success of the excitation transport was again verified by a clear bleaching of the dyes attached to the acceptor nanoparticle. Simultaneously, bleaching of the dye intercalated into the connecting DNA nanowire was also observed near the initially excited nanoparticle, *i.e.*, the donor. All the results were verified *via* control experiments also. This study demonstrates possibilities for establishing a link between nanostructures by combining the advantages of both molecular assemblies and plasmonics. Since here the donor nanoparticle was always destroyed during the initiation of the transfer, the method is limited to single use in this form. However, by further theoretical and experimental studies this can be most probably avoided and the method could be utilized in nanoscale integration, for providing a communication method between novel molecular devices equipped with parallel bottom-up fabrication capabilities. In addition to a robust and well-localized coupling, one could easily envision altering of the coupling by molecular, electrical, or optical means, thus providing a platform for actively controlled applications.

METHODS

Sample Fabrication. The buffer used in every fabrication process was 1× TBE involving 89 mM Tris base, 89 mM boric acid, and 2 mM EDTA and precisely tuned to have a pH of 8.0 by HCl. For the fluorescent staining of the λ-DNA (Fermentas GmbH, St. Leon-Rot, Germany) the SYBR green II (Molecular Probes, Eugene, OR, USA) dye was 10 times diluted in the TBE buffer to obtain a working solution (WS). All WSs were stored at 4 °C and used on the same or next day after fabrication. The staining was carried out by further diluting the SYBR green II WS by TBE by a ratio of 1:50 000 (vol) and letting it react with 4 ng/μL genomic bacteriophage λ-DNA molecules for 30 min or more. After that, the aqueous solution of the silver nanoparticles (~10^{11} particles/mL) fabricated with the recipe from ref 42, resulting in a diameter of ~40 nm and LSPR band around 417 nm, was mixed and incubated with stained λ-DNA in a ratio of 25:1 (vol) and subsequently applied as droplets onto the surface of a cleaned glass cover slide spin-coated with an 80 nm thick PMMA layer in advance. The spinning of the PMMA was done in a clean room to ensure a smooth surface and hard baked after the spinning at

180 °C. While drying of the droplet the fluorescently stained and nanoparticle-labeled λ-DNA was immobilized and stretched by a receding meniscus.[42−44] The obtained result was verified *via* fluorescent microscopy (see below and Figure 1), as well as by atomic force microscopy (Nanoscope III with a Dimension 3100 detector head from Digital Instruments, Santa Barbara, CA, USA). All the preparations were done in ambient conditions.

Experimental Setup. The experiment used a modified Observer microscope (Zeiss Inc., Jena, Germany) (see Figure 1) in ambient conditions for taking fluorescence images of the prepared sample before and after the femtosecond pulse illumination procedure. The single-photon-sensitive IXON X3 camera (Andor Inc., Belfast, Northern Ireland) was used to take a 512 × 512 pixel image from the illuminated area using an integration time of 100 ms. During this time only very weak bleaching of the dsDNA-intercalated SYBR Green II dye was observed (Figure 5). The dye was excited by ET bandpass 470/40 (Zeiss) filtered white light, and the fluorescence was measured using an HC 550/88 fluorescence filter (Zeiss) in front of the camera.

For the excitation of AgNPs a titanium/sapphire laser (Mira Optima 900-D, Coherent Inc., Santa Clara, CA, USA) delivering 100 fs long pulses at a wavelength of 800 nm and repetition rate of 76 MHz was coupled to the same Observer microscope used in fluorescent imaging. The microscope was equipped with an oil immersion objective (magnification: 63×, numerical aperture: 1.25, Zeiss) to obtain a pulse fluence of 3 mJ/cm^2. An independent measurement of the laser fluence was carried out to ensure the optimal conditions for nanoparticle excitation.[42] For the area illumination the stage scanning method using a Nano 545 3R7 stage (PI Instruments Inc., Karlsruhe, Germany) and a PI XYZ piezo controller was utilized. The scanning was done in 1 μm steps, which guarantees the excitation of the nanoparticles within the area. Irradiation time at each position varied from 500 to 1000 ms, and the fluorescence was simultaneously recorded with the CCD camera with electron multiplication enabled, thus providing even single-photon sensitivity. During the stage movements the laser beam was closed by a shutter and the camera was reset. At the end of this procedure an area of 20 μm × 20 μm was illuminated with uniform femtosecond laser fluence and a uniform dose. LabVIEW software (National Instruments, USA) was used to realize the needed synchronization between the devices.

Conflict of Interest: The authors declare no competing financial interest.

Acknowledgment. The authors thank Rainer Heintzmann and Ivana Sumanovac for help with the CCD camera and A. Ihring, K. Kandera, K. Pippardt, H. Porwol, M. Sossna, D. Horn, J. Albert, G. Schmidl, and U. Hübner for assistance with sample preparation. Financial support from Beutenberg Fellowship (MicroInter, TMWFK PE-113-1), Academy of Finland (Project Nos. 218182 and 263262), NewIndigo ERA-NET NPP2 (AQUATEST, INDIGO-DST1-012), and COST actions MP0802 and MP0803 is greatly acknowledged.

Supporting Information Available: Detailed descriptions of the fluorescent and absorption properties of the nanoparticles and the dye. Data, results, and discussion of the control experiment. This material is available free of charge *via* the Internet at http://pubs.acs.org.

REFERENCES AND NOTES

1. Seeman, N. D. DNA in a Material World. *Nature* **2003**, *421*, 427–431.
2. Rothemund, P. W. K. Folding DNA to Create Nanoscale Shapes and Patterns. *Nature* **2006**, *440*, 297–302.
3. Andersen, E. S.; Dong, M.; Nielsen, M. M.; Jahn, K.; Subramani, R.; Mamdouh, W.; Golas, M. M.; Sander, B.; Stark, H.; Oliveira, C. L. P.; *et al*. Self-Assembly of a Nanoscale DNA Box with a Controllable Lid. *Nature* **2009**, *459*, 73–76.
4. Douglas, S. M.; Dietz, H.; Liedl, T.; Högberg, B.; Graf, F.; Shih, W. M. Self-Assembly of DNA into Nanoscale Three-Dimensional Shapes. *Nature* **2009**, *459*, 414–418.
5. Okahata, Y.; Kobayashi, T.; Tanaka, K.; Shimomura, M. Anisotropic Electric Conductivity in an Aligned DNA Cast Film. *J. Am. Chem. Soc.* **1998**, *120*, 6165–6166.
6. Kelley, S. O.; Barton, J. K. Electron Transfer Between Bases in Double Helical DNA. *Science* **1999**, *283*, 375–381.
7. Fink, H.-W.; Schönenberger, C. Electrical Conduction Through DNA Molecules. *Nature* **1999**, *398*, 407–410.
8. Porath, D.; Bezryadin, A.; De Vries, S.; Dekker, C. Direct Measurement of Electrical Transport through DNA molecules. *Nature* **2000**, *403*, 635–638.
9. Endres, R. G.; Cox, D. L.; Singh, R. R. P. *Colloquium:* The Quest for High-Conductance DNA. *Rev. Mod. Phys.* **2004**, *76*, 195–214.
10. Mallajosyula, S. S.; Pati, S. K. Toward DNA Conductivity: A Theoretical Perspective. *J. Phys. Chem. Lett.* **2010**, *1*, 1881–1894.
11. Mahapatro, A. K.; Lee, G. U.; Jeong, K. J.; B. Janes, D. B. Stable and Reproducible Electronic Conduction through DNA Molecular Junctions. *Appl. Phys. Lett.* **2009**, *95*, 083106.
12. Adessi, Ch.; Walch, S.; Anantram, M. P. Environment and Structure Influence on DNA Conduction. *Phys. Rev. B* **2003**, *67*, 081405(R).
13. Linko, V.; Paasonen, S.-T.; Kuzyk, A.; Törmä, P.; Toppari, J. J. Characterisation of the Conductance Mechanisms of the DNA Origami by AC Impedance Spectroscopy. *Small* **2009**, *5*, 2382–2386.
14. Linko, V.; Leppiniemi, J.; Paasonen, S.-T.; Hytönen, V. P.; Toppari, J. J. Defined-Sized DNA Triple Crossover Construct for Molecular Electronics: Modification, Positioning and Conductance Properties. *Nanotechnology* **2011**, *22*, 275610.
15. Xu, B.; Zhang, P.; Li, X.; Tao, N. Direct Conductance Measurement of Single DNA Molecules in Aqueous Solution. *Nano Lett.* **2004**, *4*, 1105–1108.
16. Genereux, J. C.; Barton, J. K. Mechanisms for DNA Charge Transport. *Chem. Rev.* **2010**, *110*, 1642–1662.
17. Holmlin, R. E.; Dandliker, P. J.; Barton, J. K. Charge Transfer through the DNA Base Stack. *Angew. Chem., Int. Ed.* **2004**, *36*, 2714–2730.
18. Rakitin, A.; Aich, P.; Papadopoulos, C.; Kobzar, Y.; Vedeneev, A. S.; Lee, J. S.; Xu, J. M. Metallic Conduction through Engineered DNA: DNA Nanoelectronic Building Blocks. *Phys. Rev. Lett.* **2001**, *86*, 3670–3673.
19. Aich, P.; Labiuk, S. L.; Tari, L. W.; Delbaere, L. J. T.; Roesler, W. J.; Falk, K. J.; Steer, R. P.; Lee, J. S. M-DNA: A Complex Between Divalent Metal Ions and DNA which Behaves as a Molecular Wire. *J. Mol. Biol.* **1999**, *294*, 477–485.
20. Calzolari, A.; Di Felice, R.; Molinari, E.; Garbesi, A. G-Quartet Biomolecular Nanowires. *Appl. Phys. Lett.* **2002**, *80*, 3331–3333.
21. Phillips, K.; Dauter, Z.; Morchie, A. I. H.; Lilley, D. M. J.; Luisi, B. The Crystal Structure of a Parallel-Stranded Guanine Tetraplex at 0.95 Å Resolution. *J. Mol. Biol.* **1997**, *273*, 171–182.
22. Moth-Poulsen, K.; Bjørnholm, T. Molecular Electronics with Single Molecules in Solid-State Devices. *Nat. Nanotechnol.* **2009**, *4*, 551–556.
23. Debreczeny, M. P.; Svec, W. A.; Wasielewski, M. R. Optical Control of Photogenerated Ion Pair Lifetimes: An Approach to a Molecular Switch. *Science* **1996**, *274*, 584–587.
24. Battacharyya, S.; Kibel, A.; Kodis, G.; Liddell, P. A.; Gervaldo, M.; Gust, D.; Lindsay, S. Optical Modulation of Molecular Conductance. *Nano Lett.* **2011**, *11*, 2709–2714.
25. Zayats, A. V.; Smolyaninov, I. I.; Maradudin, A. A. Nano-Optics of Surface Plasmon Polaritons. *Phys. Rep.* **2005**, *408*, 131–314.
26. Raether, H. *Surface Plasmons on Smooth and Rough Surfaces and Grattings*; Springer-Verlag: New York, 1988.
27. Grésillon, S.; Aigouy, L.; Boccara, A. C.; Rivoal, J. C.; Quelin, X.; Desmarest, C.; Gadenne, P.; Shubin, V. A.; Sarychev, A. K.; Shalaev, V. M. Experimental Observation of Localized Optical Excitations in Random Metal-Dielectric Films. *Phys. Rev. Lett.* **1999**, *82*, 4520–4523.
28. Messinger, B. J.; Vonraben, K. U.; Chang, R. K.; Barber, P. W. Local-Fields at the Surface of Noble-Metal. *Phys. Rev. B* **1981**, *24*, 649–657.

29. Hüttmann, G.; Radt, B.; Serbin, J.; Lange, B. I.; Birngruber, R. High Precision Cell Surgery with Nanoparticles? *Med. Laser Appl.* **2002**, *17*, 9–14.
30. Hirsch, L. R.; Stafford, R. J.; Bankson, J. A.; Sershen, S. R.; Rivera, B.; Price, R. E.; Hazle, J. D.; Halas, N. J.; West, J. L. Nanoshell-Mediated Near-Infared Thermal Therapy of Tumors Under Magnetic Guidance. *Proc. Natl. Acad. Sci. U. S. A.* **2003**, *100*, 13549–13554.
31. Csaki, A.; Garwe, F.; Steinbrück, A.; Maubach, G.; Festag, G.; Weise, A.; Riemann, I.; König, K.; Fritzsche, W. A Parallel Approach for Subwavelength Molecular Surgery Using Gene-Specific Positioned Metal Nanoparticles as Laser Light Antennas. *Nano Lett.* **2007**, *7*, 247–253.
32. Kogan, M. J.; Bastus, N. G.; Amigo, R.; Grillo-Bosch, D.; Ataya, E.; Turiel, A.; Labarta, A.; Giralt, E.; Puntes, V. F. Nanoparticle-Mediated Local and Remote Manipulation of Protein Aggregation. *Nano Lett.* **2006**, *6*, 110–115.
33. Garwe, F.; Bauerschäfer, U.; Csaki, A.; Steinbrück, A.; Ritter, K.; Bochmann, A.; Bergmann, J.; Weise, A.; Akimov, D.; Maubach, G. Optically Controlled Thermal Management on the Nanometer Length Scale. *Nanotechnology* **2008**, *19*, 055207.
34. Kupersztych, J.; Monchicourt, P.; Raynaud, M. Ponderomotive Acceleration of Photoelectrons in Surface-Plasmon-Assisted Multiphoton Photoelectric Emission. *Phys. Rev. Lett.* **2001**, *86*, 5180–5183.
35. Kupersztych, J.; Raynaud, M. Anomalous Multiphoton Photoelectric Effect in Ultrashort Time Scales. *Phys. Rev. Lett.* **2005**, *95*, 147401.
36. Döppner, T.; Fennel, T.; Radcliffe, P.; Tiggesbaumker, J.; Meiwes-Broer, K. H. Ion and Electron Emission from Silver Nanoparticles in Intense Laser Fields. *Phys. Rev. A* **2006**, *73*, 031202(R).
37. Bharadwaj, P.; Deutsch, B.; Novotny, L. Optical Antennas. *Adv. Opt. Photonics* **2009**, *1*, 438–483.
38. Merlein, J.; Kahl, M.; Zuschlag, A.; Sell, A.; Halm, A.; Boneberg, J.; Leiderer, P.; Leitenstorfer, A.; Bratschitsch, R. Nanomechanical Control of an Optical Antenna. *Nat. Photonics* **2008**, *2*, 230–233.
39. Kuzyk, A.; Pettersson, M.; Toppari, J. J.; Hakala, T. K.; Tikkanen, H.; Kunttu, H.; Törmä, P. Molecular Coupling of Light with Plasmonic Waveguides. *Opt. Express* **2007**, *15*, 9908–9917.
40. Giannini, V.; Fernández-Domínguez, A. I.; Heck, S. C.; Maier, S. A. Plasmonic Nanoantennas: Fundamentals and Their Use in Controlling the Radiative Properties of Nanoemitters. *Chem. Rev.* **2011**, *111*, 3888–3912.
41. Stockman, M. I. Nanoplasmonics: Past, Present, and Glimpse into Future. *Opt. Express* **2011**, *19*, 22029–22106.
42. Wirth, J.; Garwe, F.; Hähnel, G.; Csáki, A.; Jahr, N.; Stranik, O.; Paa, W.; Fritzsche, W. Plasmonic Nanofabrication by Long-Range Excitation Transfer *via* DNA Nanowire. *Nano Lett.* **2011**, *11*, 1505–1511.
43. Bensimon, D.; Simon, A. J.; Croquette, V.; Bensimon, A. Stretching DNA with a Receding Meniscus: Experiments and Models. *Phys. Rev. Lett.* **1995**, *74*, 4754–4757.
44. Maubach, G.; Csáki, A.; Born, D.; Fritzsche, W. Controlled Positioning of a DNA Molecule in an Electrode Setup Based on Self-Assembly and Microstructuring. *Nanotechnology* **2003**, *14*, 546–550.
45. Maubach, G.; Fritzsche, W. Precise Positioning of Individual DNA Structures in Electrode Gaps by Self-Organization onto Guiding Microstructures. *Nano Lett.* **2004**, *4*, 607–611.
46. Hutter, E.; Fendler, J. H.; Roy, D. Surface Plasmon Resonance Studies of Gold and Silver Nanoparticles Linked to Gold and Silver Substrates by 2-Aminoethanethiol and 1,6-Hexanedithiol. *J. Phys. Chem. B* **2001**, *105*, 11159–11168.
47. Scharte, M.; Porath, R.; Ohms, T.; Aeschlimann, M.; Lamprecht, B.; Ditlbacher, H.; Aussenegg, F. R. Lifetime and Dephasing of Plasmons in Ag-Nanoparticles. *SPIE* **2001**, *4456*, 14–21.
48. Boman, F. C.; Musorrafiti, M. J.; Gibbs, J. M.; Stepp, B. R.; Salazar, A. M.; Nguyen SonBinh, T.; Geiger, F. M. DNA Single Strands Tethered to Fused Quartz/Water Interfaces Studied by Second Harmonic Generation. *J. Am. Chem. Soc.* **2005**, *127*, 15368–15369.
49. Stokes, G. Y.; Gibbs-Davis, J. M.; Boman, F. C.; Stepp, B. R.; Condie, A. G.; Nguyen, S. T.; Geiger, F. M. Making "Sense" of DNA. *J. Am. Chem. Soc.* **2007**, *129*, 7492–7493.
50. Boman, F. C.; Gibbs-Davis, J. M.; Heckman, L M.; Stepp, B. R.; Nguyen, S. T.; Geiger, F. M. DNA at Aqueous/Solid Interfaces: Chirality-Based Detection *via* Second Harmonic Generation Activity. *J. Am. Chem. Soc.* **2009**, *131*, 844–848.
51. Szabó, A.; Wang, Y.; Lee, S. A.; Simon, H. J.; Rupprecht, A. Optical Third Harmonic Generation Study of the Hydration of DNA Films. *Biophys. J.* **1993**, *65*, 2656–2660.
52. Eleftherion, E.; Antonakopoulos, T.; Binning, G. K.; Cherubini, G.; Despont, M.; Dholakia, A.; Dürig, U.; Lantz, M. A.; Potidis, H.; Rothuizen, H. E.; Vettiger, P. Millipede—A MEMS-Based Scanning-Probe Data Storage System. *IEEE Trans. Magn.* **2003**, *39*, 938–945.
53. Tong, L.; Gattass, R. R.; Ashcom, J. B.; He, S.; Lou, J.; Shen, M.; Maxwell, I.; Mazur, E. Subwavelength-Diameter Silica Wires for Lowloss Optical Wave Guiding. *Nature* **2003**, *426*, 816–819.
54. Trifonov, A.; Raytchev, M.; Buchvarov, I.; Rist, M.; Barbaric, J.; Wagenknecht, H.-A.; Fiebig, T. Ultrafast Energy Transfer and Structural Dynamics in DNA. *J. Phys. Chem. B* **2005**, *109*, 19490–19495.
55. May, V.; Kühn, O. *Charge and Energy Transfer Dynamics in Molecular Systems*; Wiley-VCH: Weinheim, 2011; pp 467—558.
56. Porath, D.; Cuniberti, G.; Di Felice, R. In *Long-Range Charge Transfer in DNA II*; Schuster, G. B., Ed.; Springer: Berlin, 2004; pp 183—227.
57. Takada, T.; Fujitsuka, M.; Majima, T. Single-Molecule Observation of DNA Charge Transfer. *Proc. Natl. Acad. Sci.* **2007**, *104*, 11179–11183.
58. Kawai, K.; Matsutani, E.; Maruyama, A.; Majima, T. Probing the Charge-Transfer Dynamics in DNA at the Single-Molecule Level. *J. Am. Chem. Soc.* **2011**, *133*, 15568–15577.